



High-Order Methods for the Numerical Simulation of Vortical and Turbulent Flows

Direct Numerical Simulation of a Gaussian acoustic wave interaction with a turbulent premixed flame

Alain Laverdant^{a,*}, Dominique Thévenin^b

^a Office National d'Études et de Recherches Aérospatiales (ONERA), 29, avenue de la Division Leclerc, BP 72, 92322 Châtillon-sous-Bagneux, France

^b Laboratory of Fluid Mechanics and Technical Flows, University of Magdeburg 'Otto von Guericke', Universitaetsplatz 2, 39106 Magdeburg, Germany

Available online 5 January 2005

Abstract

The interaction of a Gaussian negative pulse with a $H_2/O_2/N_2$ turbulent premixed flame is examined using Direct Numerical Simulation (DNS). Transport properties and chemical kinetics are described in a very detailed manner. An extended nonlinear local Rayleigh's criterion, for laminar as well as turbulent, premixed or nonpremixed flames, is proposed. Situations in which amplification or attenuation occur are listed. Calculations of a turbulent flame are then carried out with and without an acoustic wave and results are recorded at the same time. The influence of acoustic wave/turbulent flame interaction is obtained by a simple difference. It is shown that longitudinal and transverse velocity components are perturbed by the turbulent flame. Moreover, the vorticity induced by the acoustic wave is observed to be weak. Finally, Rayleigh's criterion shows that wave amplification occurs punctually. **To cite this article:** A. Laverdant, D. Thévenin, C. R. Mecanique 333 (2005).

© 2004 Académie des sciences. Published by Elsevier SAS. All rights reserved.

Résumé

Simulation Numérique Directe de l'interaction d'une onde acoustique gaussienne avec une flamme turbulente prémélangée. L'interaction d'une onde négative gaussienne avec une flamme turbulente prémélangée $H_2/O_2/N_2$ est examinée à l'aide d'une simulation directe. Les propriétés de transport et de cinétique chimique sont décrites de manière détaillée. Un critère de Rayleigh étendu au régime non linéaire, valable pour des flammes laminaires aussi bien que turbulentes, prémélangées ou de diffusion, est proposé. Les cas où il y a amplification (atténuation) sont recensés. Des simulations directes de flammes turbulentes sont ensuite effectuées avec et sans perturbations acoustiques. Les résultats sont stockés aux mêmes instants. Par simple soustraction, il est possible d'obtenir l'influence de la flamme turbulente sur le comportement de l'onde acoustique. Il est montré que les composantes de vitesse longitudinale et transversale sont perturbées par la flamme turbulente. En outre, la vorticit  induite par le transport de l'onde acoustique est faible. Finalement, le crit re de Rayleigh montre que l'amplification de l'onde est locale et situ e dans des zones de petites dimensions. **Pour citer cet article :** A. Laverdant, D. Th evenin, C. R. Mecanique 333 (2005).

* Corresponding author.

E-mail addresses: laverdan@onera.fr (A. Laverdant), Dominique.thevenin@vst.uni-magdeburg.de (D. Th evenin).

© 2004 Académie des sciences. Published by Elsevier SAS. All rights reserved.

Keywords: Computational fluid mechanics; Combustion instability; Rayleigh's criterion; Turbulent premixed flame

Mots-clés : Mécanique des fluides numérique ; Instabilité de combustion ; Critère de Rayleigh ; Flamme turbulente prémélangée

1. Introduction

The coupling between acoustic waves and heat release fluctuations, induced by a turbulent premixed flame, is a fundamental problem of great practical interest (control of combustion instability). Diverging pressure fluctuations have first been explained qualitatively by Lord Rayleigh [1–3]. He proposed this simple criterion: “... *If heat be given to the air at the moment of greatest condensation, or be taken from it at the moment of greatest rarefaction, the vibration is encouraged.* . . .” and “*vice versa*”. In a preceding paper, Laverdant and Thévenin [4] have proposed a mathematical nonlinear version of Rayleigh's formulation. This local quantitative criterion is extended to detailed chemical mechanism, multicomponent transport phenomena and turbulent fluctuations, in a direct way. A simplified derivation is proposed in the present work. The behaviour of a Gaussian acoustic wave, which propagates through a turbulent premixed flame, is considered. In order to obtain a very precise solution, a Direct Numerical Simulation (DNS) is carried out with complete chemical kinetics and transport mechanisms (the present results complete the presentation of [4]).

In this work, attention is focused on the following questions:

- Is the wave configuration modified by the spatial velocity of sound distribution?
- Does an acoustic wave still remains plane after crossing the flame front?
- Is the turbulent field perturbed by the acoustics? Is there a perturbed vorticity component?
- Where does the amplification of an acoustic wave occur for a turbulent flame?
- Does the modified Rayleigh's criterion explain what happens?

2. Direct derivation of Rayleigh's criterion

The developments of this paragraph constitute a major extension of [5–7]. The complete developments are presented in [4] using standard notations of [8].

Keeping only the essential source term due to combustion, the balance equation for the acoustic energy E takes this simple form:

$$\frac{\partial E}{\partial t} + \nabla \cdot \mathbf{F} = \frac{\gamma - 1}{\gamma p} \Pi' Q' \quad (1)$$

where: $\Pi' = (1/\gamma) \log(1 + p'/p_0)$ [9]; $(\cdot)_0$ denotes the unperturbed values and $(\cdot)'$ acoustic perturbations; Q' is the heat release fluctuation. Moreover:

$$E = \frac{1}{2} \left(\frac{\mathbf{v}'^2}{c^2} + \Pi'^2 \right) \quad (2)$$

$$\mathbf{F} = \mathbf{v}' \Pi' \quad (3)$$

$$Q' \simeq - \sum_{i=1}^N h_i \dot{w}'_i \quad (4)$$

E , \mathbf{F} are respectively the acoustic energy and the acoustic flux; c is the velocity of sound. If the right side of Eq. (1) is negative, the wave is attenuated. It is possible to take into account the direct and reverse stoichiometric

Table 1
Situations involved in Rayleigh's criterion, Eq. (5)

Π'	$-\sum_{i=1}^N h_i \dot{w}'_i$	Resulting effect
pressure fluctuation	heat release fluctuation	
> 0	> 0	amplification
> 0	< 0	attenuation
> 0	= 0	neutral
< 0	> 0	attenuation
< 0	< 0	amplification
< 0	= 0	neutral

Table 2
Flow conditions for DNS

Φ	X_{H_2}	X_{O_2}	X_{N_2}	T (K)	p (kPa)	S_I^0 (m/s)	u' (m/s)	Λ (mm)
0.7	0.28	0.2	0.52	800	101	14.6	31.85	2.51

coefficients of the R elementary reactions, along with the molar production rates \dot{w}_{ik} of species i in reaction k . This gives finally either

$$\Pi' \left(-\sum_{i=1}^N h_i \dot{w}'_i \right) < 0 \quad \text{or} \quad \Pi' \sum_{k=1}^R \left(-\sum_{i=1}^N (v''_{ik} - v'_{ik}) W_i h_i \dot{w}'_{ik} \right) < 0 \quad (5)$$

for attenuation resulting from the chemical reactions considered in the detailed mechanism. As a consequence, all species and all direct and reverse reactions are important, and the values of the species enthalpy must also be considered. The term $-\sum_{i=1}^N h_i \dot{w}'_i$ in the left expression is in fact the fluctuation of the heat release term due to chemical reactions in the temperature equation [10]. All different possible cases are summarized in Table 1.

3. Numerical method

The numerical code *parcomb* has been developed by Thévenin and coworkers [11,12]. It solves balance equations for a gaseous compressible reactive flow. Spatial derivations are respectively of order six in the field and of order four on the boundaries. Temporal integration is realized with a classical Runge–Kutta algorithm (order four). Flow at boundaries is treated with the help of the Navier–Stokes Characteristic Boundary Condition (NSCBC) technique [13], extended to take into account multicomponent thermodynamic properties [14]. Transport coefficients and chemical kinetics are treated following CHEMKIN II and TRANSPORT methods [15,16]. The code has been parallelized and widely used to investigate turbulent flames (see for example [12,17,18]).

4. Problem definition

For this DNS, we investigate a $H_2/O_2/N_2$ premixed turbulent flame in a two-dimensional flow. We choose here to reproduce as far as possible the conditions used in [19], Case 4. Flow conditions are summarized in Table 2.

The numerical domain is a square box of $L_{\text{box}} = 1.24$ cm with 501 equidistant points for the mesh grid in each direction. This leads to a spatial resolution of $\delta x = \delta y = 25$ μm , necessary to compute accurately the very stiff production of radicals like HO_2 .

We generate an initial turbulence field with an integral velocity fluctuation u' and an integral scale Λ (defined in Table 2). It is shown in [4] that this corresponds to a flamelet-like regime in the Borghi diagram.

Details of the mechanism employed for hydrogen–oxygen kinetics may be found in [20]. Nine species (H_2 , O_2 , H_2O , OH , H , O , HO_2 , H_2O_2 and N_2) and 19 reversible reactions are taken into account.

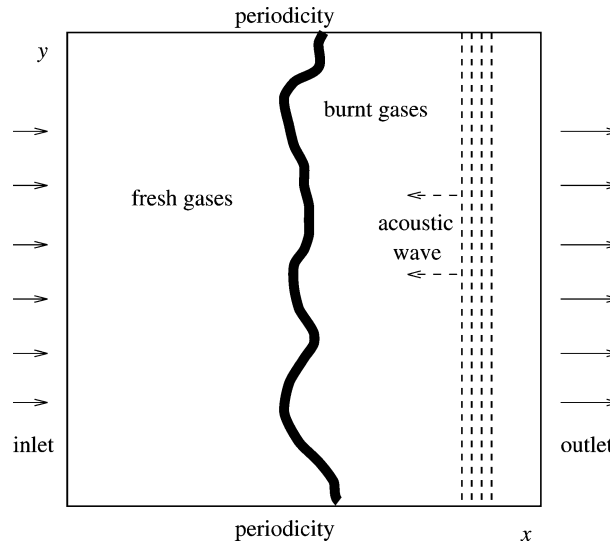


Fig. 1. Numerical configuration employed for the DNS.

The premixed laminar flame is first computed for a one-dimensional flow along the x -direction and the inlet velocity is adapted to keep the flame front in the middle of the domain. This steady solution is then transposed to a two-dimensional flow, with fresh gases on the left side and burnt gases on the right side. An isotropic two-dimensional turbulence is superposed on top of it using a von Kármán spectrum coupled with Pao correction [12,17,21]. We then compute the interaction of the initially planar flame with the turbulence field during a time equivalent to $0.72 \times (\text{turbulence time})$ (Fig. 1).

A Gaussian acoustic wave (negative pulse) is instantaneously initialized as a straight wave across the y -direction at $x_0 = 0.85L_{\text{box}}$ inside the burnt gases (near equilibrium zone). We choose this time as our new origin of time $t' = 0 \mu\text{s}$. The Gaussian acoustic perturbation has a stiffness of 60. Calculations of a turbulent flame are then carried out with and without an acoustic wave and results are recorded at the same time. The influence of acoustic wave/turbulent flame interaction is obtained by a simple difference.

5. Results

The longitudinal velocity induced by the interaction is plotted in what follows at either (a) $t' = 4 \mu\text{s}$ (Fig. 2), or (b) $t' = 7 \mu\text{s}$ (Fig. 3). This corresponds respectively to (a) a wave crossing the reaction zone; and (b) propagating in the fresh gases. In case (a), the wave will soon arrive in the fresh gases after crossing the flame and is now considerably wrinkled. It can be noticed that this wave wrinkling is related to the global flame front structure, visible, for example, in Fig. 3. A low-amplitude reflected wave on the right side of the reaction zone near the boundary ($x \simeq 8 \text{ mm}$) and a strong transmitted wave on the left side, arriving in the fresh gases are also visible. Structures with complex shapes are also observed in the longitudinal velocity field just behind the transmitted wave front. This is probably due to wave scattering by the turbulent flame [22]. In case (b), the wave has crossed the reaction zone. The wave profile is complex with multiple fronts, local amplification and large gradients. The examination of figures at successive times shows the influence of focussing effect and the importance of the velocity of sound distribution.

The transverse component of the acoustic velocity is plotted in Fig. 4 at $t' = 7 \mu\text{s}$. Alternating structures are observed, whose maximum value is relatively weak, below 1.84 m/s.

The vorticity induced by the interaction is plotted in Fig. 5 for $t' = 7 \mu\text{s}$. The unperturbed vorticity field is plotted in Fig. 6 for the same time. Small counter-rotating vortices are observed at different locations along the maximum

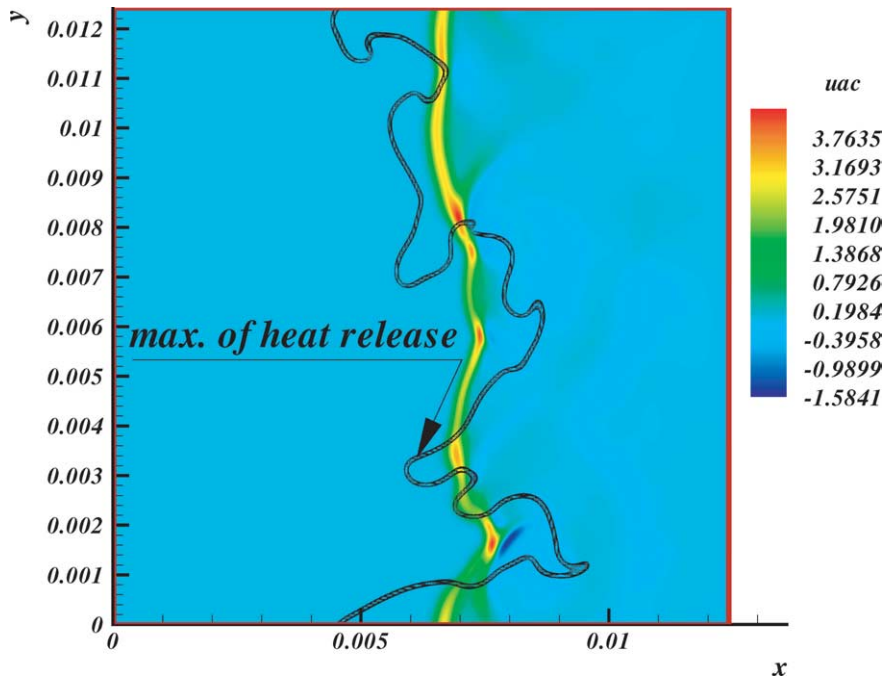


Fig. 2. Acoustically-induced longitudinal velocity field at $t' = 4 \mu\text{s}$.

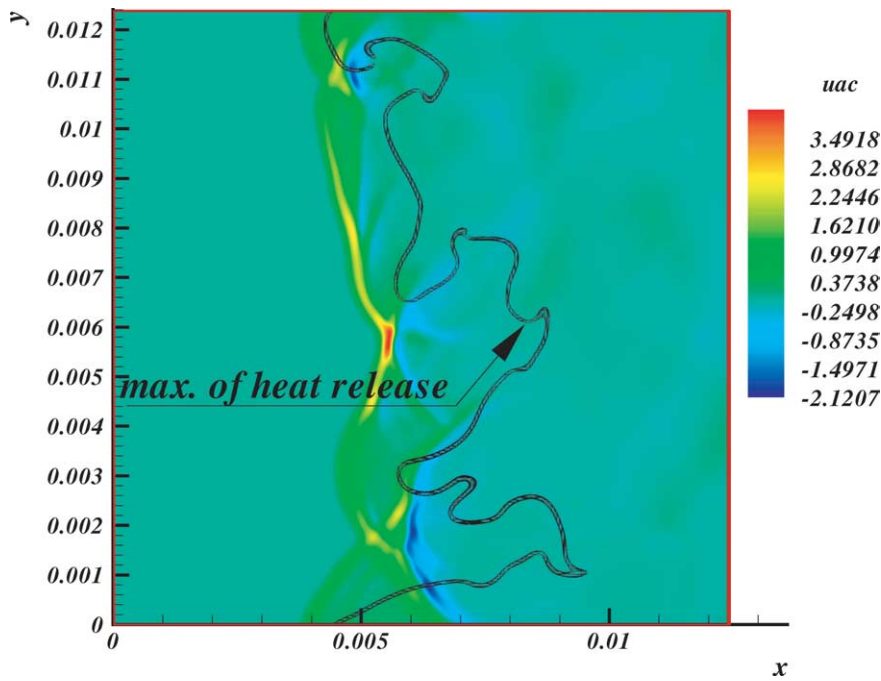


Fig. 3. Acoustically-induced longitudinal velocity field at $t' = 7 \mu\text{s}$. The maximum amplitude of the acoustic velocity is decreasing with time.

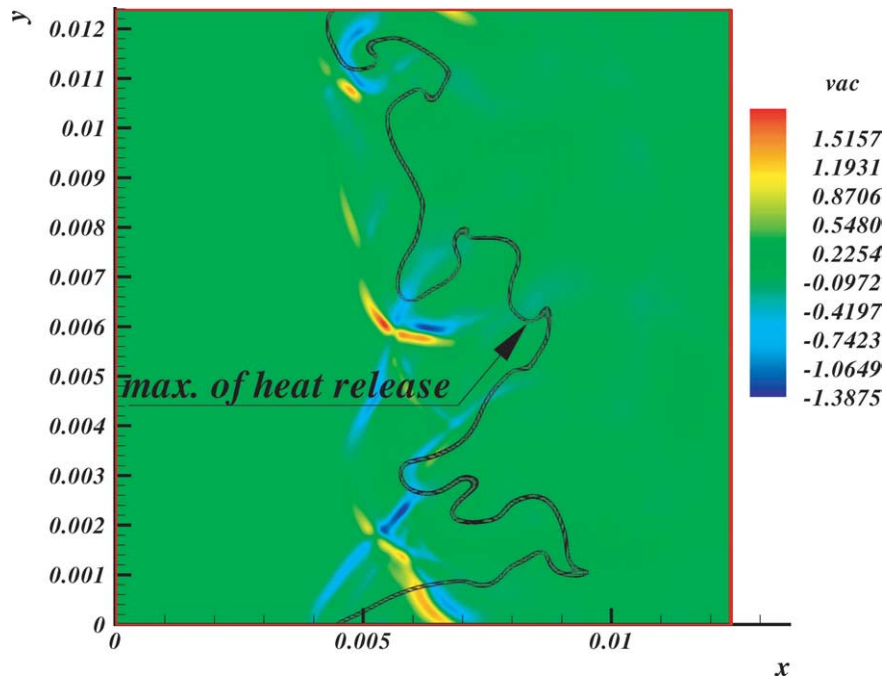


Fig. 4. Acoustically-induced transverse (y) velocity field at $t' = 7 \mu\text{s}$. Transverse velocity perturbations are observed in the fresh gases.

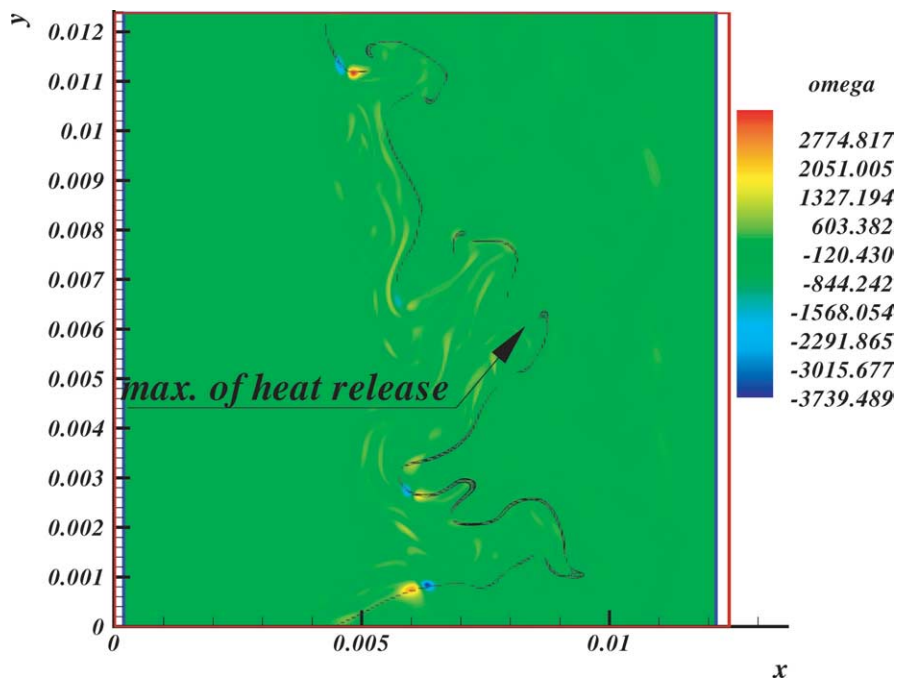


Fig. 5. Acoustically-induced vorticity field at $t' = 7 \mu\text{s}$. Small size counter-rotating vortices are observed on the maximum heat release front.

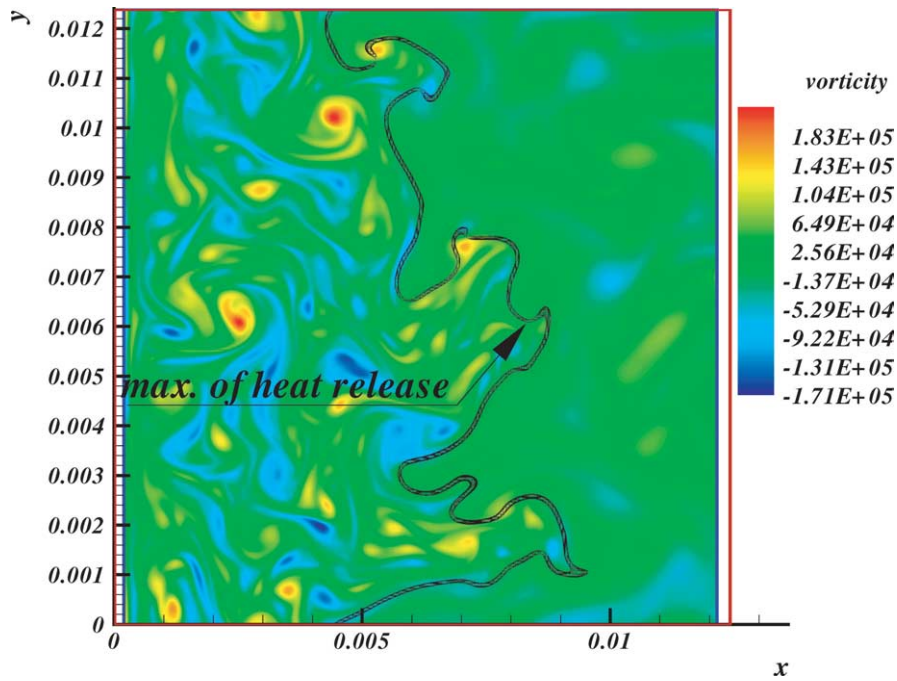


Fig. 6. Unperturbed vorticity field at $t' = 7 \mu\text{s}$. Vortices are essentially located in fresh gases, where dissipation levels are lower.

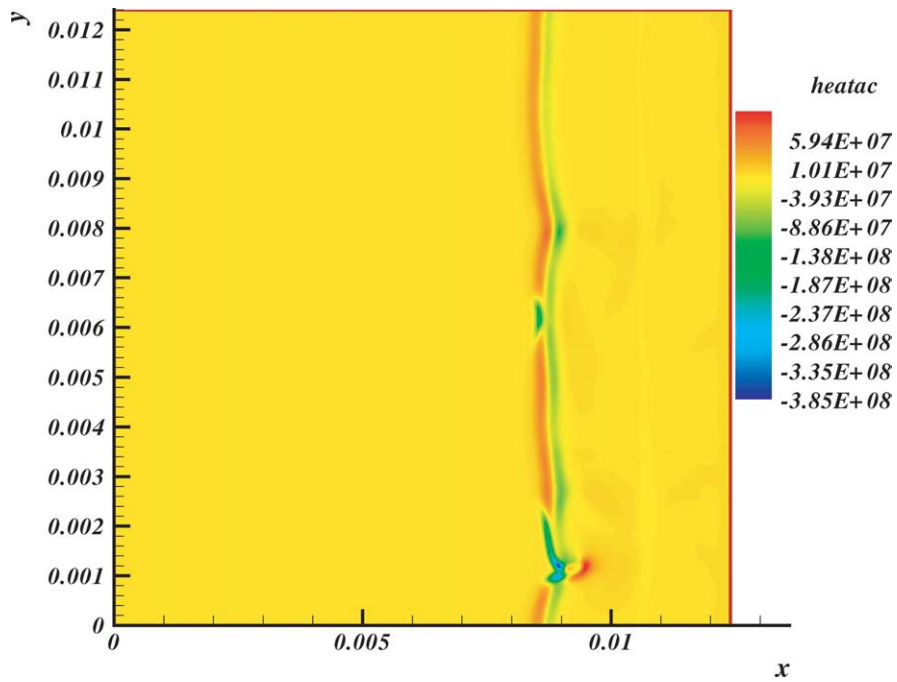


Fig. 7. Acoustically-induced heat release field at $t' = 2 \mu\text{s}$. The maximum heat release front, close to the acoustic heat release fluctuations, is not plotted for cleanliness.

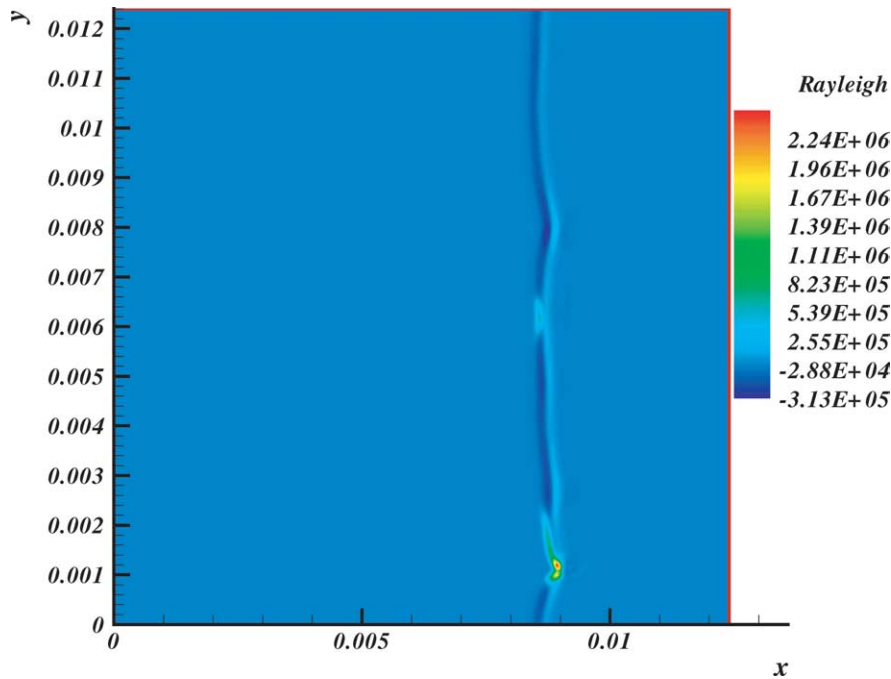


Fig. 8. Rayleigh's criterion (Eq. (5)) at $t' = 2 \mu\text{s}$. The maximum heat release front is not plotted for clearness.

heat release front. The order of magnitude of the maximum fluctuation in Fig. 6 is again very small, about 2% of the unperturbed value.

The heat release fluctuation induced by the acoustic interaction is plotted for $t' = 2 \mu\text{s}$ in Fig. 7. Similar results are available in [4]. The reaction zone is clearly observed in this last figure. Following the direction of wave propagation, the perturbations of heat release present successively negative and positive values. This situation corresponds to the beginning of the flame/wave interaction. This explains that the heat release fluctuation is only affected punctually. Here again, the induced perturbations are in fact quite weak (of the order of 1%) compared to the mean values of heat release. It is interesting to note that the fluctuations may even not be observed at all for some regions.

The modified local Rayleigh's criterion given by Eq. (5) is plotted in Fig. 8 for $t' = 2 \mu\text{s}$. As said previously, complementary results can be found in [4]. Small zones corresponding to negative or positive values are observed. Acoustic wave amplification occurs at this last place.

As a whole, the perturbations induced on heat release and vorticity by the propagation of an acoustic wave through a wrinkled turbulent premixed flame appear to be weak. Transverse velocity fluctuations are smaller than their axial counterpart, but have a significant amplitude. Focussing effects and wave scattering are observed when the acoustic wave crosses regions with large velocity of sound gradients, in the flame zone.

Our development of this modified Rayleigh's criterion shows that the wave may be amplified or damped. The influence of each species and each reaction included in the mechanism on the amplification or damping of the wave can therefore be directly explained.

6. Conclusions

The DNS of the propagation of a Gaussian wave through a $\text{H}_2/\text{O}_2/\text{N}_2$ turbulent premixed flame has given the following results:

- A planar wave is scattered by the inhomogeneous velocity of sound distribution. The wave is wrinkled after its passage through the flame front and transverse velocity component appear in fresh gases.
- A weak component of vorticity, induced by acoustic wave, is observed close to the reactive zone. This perturbation is, for a premixed turbulent flame, of negligible importance. The amplification of the acoustic wave occurs locally where focussing effects are sensitive and where Rayleigh's criterion is positive.

The present results and those of [4] give a new insight of wave amplification by turbulent premixed flames. The identification of the main species and reactions leading to attenuation is in progress. Applications for active control of combustion instability now seem possible.

Acknowledgements

This work has received a financial support of ONERA. Discussions with Drs Giovangigli, Bendahkhia and Mareschal de Charentenay have been appreciated.

References

- [1] J.W.S. Rayleigh, *Nature* 18 (1878) 319.
- [2] J.W.S. Rayleigh, *The Theory of Sound*, vol. II, Dover, New York, NJ, 1945, p. 226.
- [3] G.H. Markstein (Ed.), *Nonsteady Flame Propagation*, Pergamon Press, Paris, 1964.
- [4] A. Laverdant, D. Thévenin, Interaction of a Gaussian acoustic wave with a turbulent premixed flame, *Combust. Flame* 134 (1–2) (2003) 11–19.
- [5] S. Kotake, On the combustion noise related to chemical reactions, *J. Sound Vib.* 42 (3) (1975) 399–410.
- [6] A. Laverdant, T. Poinsot, S.M. Candel, Influence of the mean temperature field on the acoustic mode structure in a dump combustor, *J. Propul. Power* 2 (2) (1985) 134–144.
- [7] A. Laverdant, *Contribution à l'étude des instabilités de combustion des foyers aérobies*, Thèse d'État, University of Rouen, 1991.
- [8] F.A. Williams, *Combustion Theory*, second ed., Benjamin Cummings, Menlo Park, CA, 1985.
- [9] A.S. Monin, A.M. Yaglom, *Statistical Fluid Mechanics: Mechanics of Turbulence*, MIT Press, Cambridge, MA, 1979.
- [10] T. Poinsot, D. Veynante, *Theoretical and Numerical Combustion*, Edwards, Philadelphia, PA, 2001.
- [11] D. Thévenin, F. Behrendt, U. Maas, B. Przywara, J. Warnatz, Development of a parallel direct simulation code to investigate reactive flows, *Comput. Fluids* 25 (5) (1996) 485–496.
- [12] D. Thévenin, E. van Kalmthout, S. Candel, Two-dimensional direct numerical simulations of turbulent diffusion flames using detailed chemistry, in: J.P. Chollet, P.R. Voke, L. Kleiser (Eds.), *Direct and Large-Eddy Simulation II*, Kluwer Academic, 1997, pp. 343–354.
- [13] T. Poinsot, S.K. Lele, Boundary conditions for direct simulation of compressible viscous flows, *J. Comput. Phys.* 101 (1992) 104–129.
- [14] M. Baum, T. Poinsot, D. Thévenin, Accurate boundary conditions for multicomponent reactive flows, *J. Comput. Phys.* 116 (1994) 247–261.
- [15] R.J. Kee, J.A. Miller, T.H. Jefferson, Chemkin: a general-purpose, problem-independent, transportable, Fortran chemical kinetics code package, Sandia Tech. Report SAND80-8003, 1980.
- [16] R.J. Kee, J. Warnatz, J.A. Miller, A Fortran computer code package for the evaluation of gas-phase viscosities, conductivities, and diffusion coefficients, Sandia Tech. Report SAND83-8209, 1983.
- [17] R. Hilbert, D. Thévenin, Autoignition of turbulent non-premixed flames investigated using direct numerical simulations, *Combust. Flame* 128 (1–2) (2002) 22–37.
- [18] U. Maas, D. Thévenin, Correlation analysis of direct numerical simulation data of turbulent non-premixed flames, in: *Twenty-Seventh Symposium (International) on Combustion*, The Combustion Institute, Pittsburgh, 1998, pp. 1183–1189.
- [19] M. Baum, T. Poinsot, D.C. Haworth, N. Darabiha, Direct numerical simulation of $H_2/O_2/N_2$ flames with complex chemistry in two-dimensional turbulent flows, *J. Fluid Mech.* 281 (1994) 1–32.
- [20] J.A. Miller, R.E. Mitchell, M. Smooke, R.J. Kee, Toward a comprehensive chemical kinetic mechanism for the oxidation of acetylene: comparison of model predictions with results from flame and shock tube experiments, in: *Nineteenth Symposium (International) on Combustion*, The Combustion Institute, Pittsburgh, 1982, pp. 181–196.
- [21] J.O. Hinze, *Turbulence*, second ed., McGraw-Hill, 1975.
- [22] T. Lieuwen, Theory of high frequency acoustic wave scattering by turbulent flames, *Combust. Flame* 126 (2001) 1489–1505.